Spatial-reuse TDMA for Large Scale Underwater Acoustic Multi-hop Grid Networks

Jianyu Zhang, Filippo Campagnaro, Michele Zorzi

***Abstract*—In contrast to terrestrial wireless network, where the propagation delay is almost negligible when compared to the packet duration (i.e., the duration of the signal carrying a packet), in underwater acoustic networks it is not rare to observe a propagation delay equal to, or even greater than, the packet duration, as the signal travels at the speed of sound that is orders of magnitude smaller than the speed of light. On the one hand, this phenomenon makes carrier sense-based Medium Access Control (MAC) protocols, such as Carrier Sense Multiple Access (CSMA), almost ineffective in underwater acoustic networks [1]. In fact, CSMA outperforms other contention-based protocols such as Aloha and Slotted Aloha only if its vulnerable time, that in CSMA is equal to the propagation delay, is at least 100 times smaller than the packet duration. Moreover, the standard Time Division Multiple Access (TDMA) is very inefficient, as each time slot should account for a guard time equal to the maximum propagation delay to avoid collisions between consecutive slots. On the other hand, the large propagation delay can be exploited by scheduling simultaneous transmissions between adjacent nodes without causing collisions at the receiver. In this paper we design a MAC scheme that leverages on the propagation delay and on the near-far interference to maximize the packet transmissions in large underwater acoustic grid networks, and we compare its performance with other MAC protocols implemented in the DESERT Underwater Framework [2].**

***Index Terms*—Underwater networks, underwater internet of things, MAC layer, spatial-reuse TDMA.**

I. Introduction

With the development of various technologies in marine engineering, the application of underwater acoustic communication has gradually shifted from military applications to industrial and civilian applications [3]. The application scenarios of underwater communication networks are advancing, demanding higher performance for underwater real-time data transmission. Various frequency bands for underwater acoustic communication are heavily exploited for high-performance acoustic transducer products [4]–[6]. However, there are few examples of multi-node large-scale underwater acoustic network applications, as low data rate, large delay, multi-node interference, etc., restrict the networking capabilities of underwater acoustic communication equipment. The MAC protocol is the first bottleneck from communication to network. MAC protocol design in underwater acoustic networks [1] rely on fundamentally different assumptions than terrestrial radio MAC protocol design, where the propagation delay is negligible. In contrast, in underwater acoustic networks, the large propagation delay cannot be neglected and, together with the limited bandwidth and unstable connection, is usually the main cause of throughput degradation. However, if the MAC protocol is designed properly, it can leverage on the propagation delay to increase the overall throughput of the network by scheduling simultaneous transmissions.

J. Zhang (email: jianyu.zhang@studenti.unipd.it), F. Campagnaro (email: campagn1@dei.unipd.it), and M. Zorzi (email: zorzi@dei.unipd.it), are with the Department of Information Engineering, University of Padova, Italy.

This work has been partially supported by the European Union - FSE REACT EU, PON Research and Innovation 2014-2020 (DM 1062/2021) and by the European Union under the Italian National Recovery and Resilience Plan (NRRP) of NextGenerationEU, partnership on "Telecommunications of the Future" (PE0000001 - program "RESTART") and by China Scholarship Council (CSC) under the Grant CSC N°202008220156.

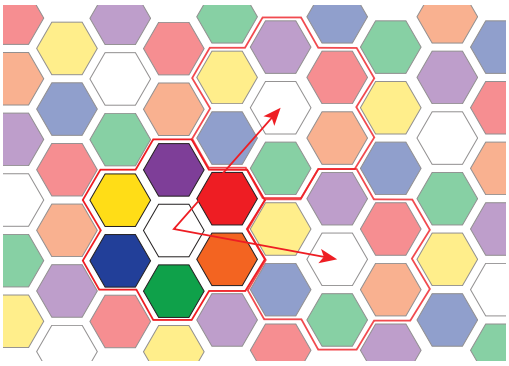

Fig. 1. Coloring solution for cellular grid networks.

The idea of taking advantage of large propagation delays has been considered in many studies [7]–[9], that usually focus on small underwater networks. Conversely, in this work we consider a large scale grid sensor network deployment like the one depicted in Figure 1. In fact, in large scale sensor networks, the grid deployment provides the full coverage of a wide area, making it suitable for Intelligence gathering, Surveillance and Reconnaissance (ISR) applications [10]. Moreover, a grid network topology also has good cyclic symmetry, which makes it suitable to reduce the complexity of resource allocation problems. Nevertheless, such grid networks have to face the challenges of underwater acoustic sensor networks: hidden terminals, exposed terminals, and more serious multi-hop interference than in terrestrial wireless networks [11].

Coloring of Unit Disc graphs solutions can be applied to the channel assignment problem [12]. In this paper, we introduce a Spatial-reuse TDMA protocol for large scale underwater acoustic grid networks. We take advantage of propagation delay to allow every node to choose one neighbor to transmit to each other in the same time slot. In order to find the optimal schedule, we divide this problem into two phases, namely, graph coloring and schedule planning. Specifically, we color the nodes in the network with a sufficiently small number of colors. Nodes with the same color (Figure 1) have the same schedule to transmit and receive. Then we search for the optimal schedule that minimizes the number of idle slots

and may even allow nodes with different colors to transmit in the same time slot as soon as the packet reception is ensured to be successful.

In this paper we describe our scheduling solution, evaluating it in a realistic scenario by means of the DESERT Underwater network simulator [2]. The remainder of the paper is organized as follows. In Section II, we describe the assumptions and system model. In Section III, we present coloring and scheduling solutions that take advantage of propagation delay, as well as some improved solutions to mitigate the multi-hop interference for large scale and heavy traffic scenarios. In Section IV, we present the simulation scenario and results. Finally, in Section V, we conclude the paper and discuss future work.

II. System Model and Parameters Description

TABLE I
Parameters Description

Name	Description
N	number of nodes
D	distance between adjacent nodes
c	speed of sound underwater
T	slot length, equal to the propagation delay
t_{pkt}	packet duration
t_g	guard time
k	number of nodes in a cell

We consider a cellular grid deployed network with N half-duplex omnidirectional transceivers in communication range only with the adjacent nodes. We group the nodes in cells of k nodes, and D is the average distance between adjacent nodes: we consider the nodes to be anchored and only float around a small range $d \ll D$. To provide flexibility to upper layer and different applications, every node is equal in transmission power and energy consumption and transmits to other nodes with equal probability. The network is a multi-hop relay network with unicast packets. Nodes only send to or receive from one adjacent neighbor node at the beginning of a time slot. We consider a speed of sound in the water c = 1500 m/s, we set the slot length $T = D/c$ and we consider a guard time t_g as a fraction of the slot T. The packet duration $t_{pkt} < T$ is set to $t_{pkt} = T - t_g$. The list of parameters used in our system model is summarized in Table II. We consider the nodes to be synchronized upon deployment and equipped with a precise clock, such as an atomic clock [13] or an oven-controlled crystal oscillator [14]. Alternatively, to reduce the deployment cost, the nodes can run a synchronization algorithm [15] every hour. The nodes know the position and ID of their neighbors upon deployment. Each node runs a cyclic schedule to send and receive packets. Specifically, in each frame, a node has one slot to transmit and one slot to receive for each of its neighbors. The schedule may also include idle slots, where nodes remain silent.

III. Cell Coloring Schedule for Multi-hop Grid Networks

Our algorithm to solve the Spatial reuse TDMA for underwater acoustic multi-hop grid networks consists of two phases.

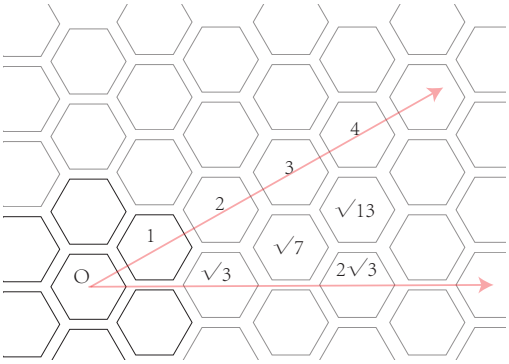

Fig. 2. Distance between nodes in cellular grid networks.

First, we assign a color to each node making sure its neighbors all have different colors among them and from itself. Then, we plan the schedule taking advantage of the propagation delay. Nodes with the same color use the same schedule to achieve spatial reuse.

A. Cell Coloring Algorithm

Our goal is to color the given grid topology with scalability and spatial reuse. On that note, we consider such algorithm to find a cell structure that can scale in the grid and each node within the cell has the same distance with the translational symmetry node of an adjacent cell. We call this distance as the distance between adjacent cells. Denote the area occupied by a node as A and the distance between adjacent nodes as D. We show the distance between nodes in the grid topology in Figure 2. For a cell of k nodes, the area a cell occupies is $k \cdot A$. the distance between adjacent cells is $\sqrt{k} \cdot D$. Take any certain translational symmetry nodes in all the cells, they form a $\sqrt{k}$ scaled grid.

In a linear topology, the network scales along the line as it has only one dimension. In two-dimensional grid topology, the network can scale along two linearly independent basis vectors. The position of every node in a grid network can be expressed as a linear combination of the two basis vectors. To locate the translational symmetry nodes grid as the cell grid, we take two adjacent translational symmetry nodes of a certain node that these three nodes are not on the same straight line. The relative position of these two adjacent translational symmetry nodes can be the new basis vectors to form the cell grid. Once we locate the cell grid in the whole grid network, the position of other nodes in the cell can be expressed as the vector of the cell combined with the vector within the cell. We color our k node cells with k different colors and repeat the same color with translational symmetry nodes. This coloring provides the whole grid colored with k different colors and nodes with the same color have the same distance forming a larger grid. For different grid topologies, an inner node can have a different number of neighbors. For a cellular grid network, an inner node has 6 neighbors. To ensure in a cell every node has different colored neighbors, the least number of colors is 7. 7 colors give us the availability of arranging the arrival time of every 1 hop neighbor. In the figure above, we

notice that there exists such distance of nodes $\sqrt{7}$ that meets the above 7 color cell condition. We show the 7 color cell coloring solution in Figure 1.

B. Scheduling for n color TDMA taking advantage of propagation delay

While the coloring solution, where only nodes with the same color are allowed to transmit at the same time, is sufficient to allocate the slots in a traditional spatial reuse TDMA (STDMA), we can take advantage of the propagation delay to allow nodes with two different colors to transmit simultaneously and receive simultaneously, as long as the packet duration is less than the propagation delay. It saves the extra guard time for propagation delay in traditional TDMA which is usually greater than or equal to the maximum propagation delay between nodes in range.

In fact we set two colors, for example blue (B) and green (G), to transmit in the same time slot to each other. If B transmits to G and G transmits to B in the same time slot t_i, given that $t_{pkt} < T$ the packets are correctly received at the destinations. While, in time slot t_{i+1}, B and G are receiving the packets from each other, the next pair of colors yellow (Y) and white (W) can transmit to each other without causing collisions. To ensure fairness, in one complete time frame every node transmits to and receives from all the neighbor nodes one packet. For a lattice grid, every inner node has 4 neighbors. We need 5 colors to form the cell. In a 5-color schedule, we have C(5, 2) = 10 transceiver pairs. To arrange them in a schedule, we build a graph of the 10 pairs, and connect pairs without common nodes. The resulting graph is a Petersen Graph [16]: such graph does not have a Hamiltonian cycle, but it does have Hamiltonian paths and can be divided into two graphs of 5 nodes with a Hamiltonian cycle. Figure 3 shows the 10 transmission pairs in Petersen Graph. Vertex AB represents that the transmission pairs from color A to Color B and from Color B to Color A can be scheduled in the same slot. Edge AB-CE means that the transmission pairs AB and the transmission pair CE can be scheduled right after or right before the transmission of one another without conflict. With the Hamiltonian path, we can arrange the transmission schedule along the path and add one extra slot as guard time to correctly receive the last transmission without conflict or collision with the first transmission of the next frame.

For a 6-neighbor cellular grid network, we can easily build a graph with 7 color transmission pairs and find a Hamiltonian cycle [16]. We show in Table II a solution of our scheduling problem, where the item $k, t_i = v$ corresponds to the schedule for nodes with color k in time slot t_i. The value v is positive if in time slot t_i nodes with color k are transmitting to destinations with color v, and negative if nodes with color k are receiving from nodes with color $|v|$.

As the scale of grid becomes larger, the interference from non adjacent neighbors becomes heavier. To lower the interference from two hop neighbors, we need control over two hop neighbors. We propose a 13 color cell coloring solution and try to find a better way to arrange the arrival of transmission

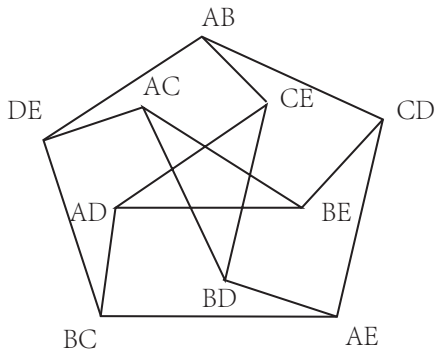

Fig. 3. 10 transmission pairs in Petersen Graph.

TABLE II
7 COLOR HAMILTONIAN CYCLIC SCHEDULING TABLE

Color\Slot	1	2	3	4	5	...	21
1	2	-2	0	7	-7	...	0
2	1	-1	0	0	3	...	0
3	0	4	-4	0	2	...	0
4	0	3	-3	0	0	...	-5
5	0	0	6	-6	0	...	-4
6	-7	0	5	-5	0	...	7
7	-6	0	0	1	-1	...	6

and interference from nodes with different but controllable distance. We notice in the former figure, that there exist a distance of $\sqrt{13} \cdot D$. Such cell with a distance of adjacent cells of $\sqrt{13} \cdot D$, provide a 13 color solution and easy control of up to two hop neighbors. In Figure 4, we show the coloring solution of 13 color cell. We notice this property in this coloring solution: The nodes with certain colors are always having the same colors neighbor from the same positions. Nodes that are not neighbors are always with the same colors from the same positions with both distance of $\sqrt{3} \cdot D$ and $2 \cdot D$. Taking nodes with color 1 as an example, they are all having neighbors with color 2, 3, 4, 5, 6, 7 from specific positions. Moreover, they all have exactly one non neighbor node with color 8, 9, 10, 11, 12, 13 from $\sqrt{3} \cdot D$ away and exactly one

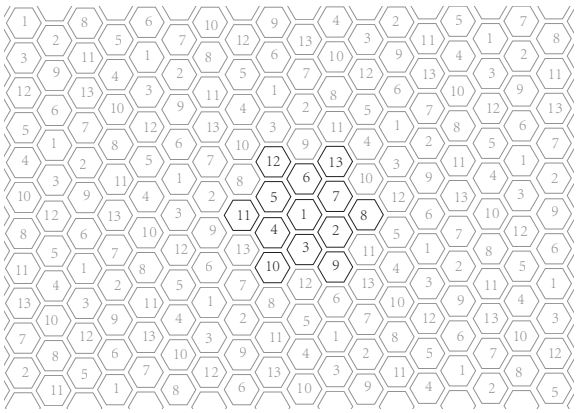

Fig. 4. 13 color cell solution

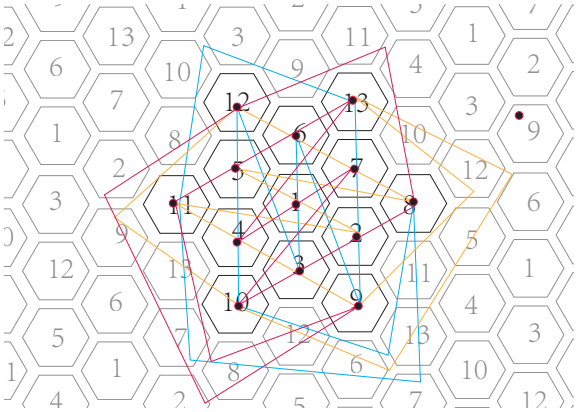

Fig. 5. 3 loops in 13 color adjacency graph.

of that from $2 \cdot D$ away. This ensures the two hop neighbor interference are only from at most two nodes with controllable time of arrival and color. Additional to a transmission pair, we can add one extra transmission from a non neighbor color nodes in the same slot and ensure that in the next slot these three receptions are safe from two hop neighbors. In the second slot, there are two different available transmission pairs and one safe transmission for each pair. To follow either solution we can achieve the same structure and have one direction to go until it forms a closed loop. Such loop consists of 26 slots. We consider the 26 cyclic and mirror symmetric variation of such loop as the same loop, there are three different loops with clear majority flow direction difference (Figure 5). Each of these three loops does not provide per link fairness nor covers all the transmission pairs equally. But we notice that they are rotationally symmetric. We connect the three loops and their mirror symmetry, adding one idle slot after the reception of the last transmission as the guard between different loops to form the frame of 168 slots. This ensures that every link repeats 6 times within a frame. In Table III, we show part of the scheduling solution.

TABLE III
7 COLOR HAMILTONIAN CYCLIC SCHEDULING TABLE

Color\Slot	1	2	3	4	...	168
1	2	-2	-5	5	...	0
2	1	-1	-11	0	...	0
3	0	0	0	12	...	0
4	0	0	0	0	...	0
5	0	1	8	-8	...	0
6	0	0	0	0	...	0
7	0	0	-13	8	...	0
8	0	0	5	-5	...	0
9	0	0	0	-13	...	0
10	0	-12	0	0	...	0
11	0	2	0	0	...	0
12	10	0	0	0	...	0
13	0	7	9	0	...	0

IV. RESULTS

A. Simulation scenario and settings

In order to evaluate our solution in a realistic environment, we simulate the proposed schedule with the DESERT Underwater simulation framework [2] and compare its performance against CSMA-Aloha, i.e., a MAC layer that does carrier sensing in underwater acoustic networks. However, given the long propagation delay, it performs like Aloha. We simulate the proposed two scheduling solutions with similar setup and different numbers of nodes, i.e., 9 nodes and 100 nodes. Node positions are shown in Figure 6 and Figure 7. The distance between neighboring grid nodes D is set to 1500 m, therefore the propagation delay between neighbors is 1 s.

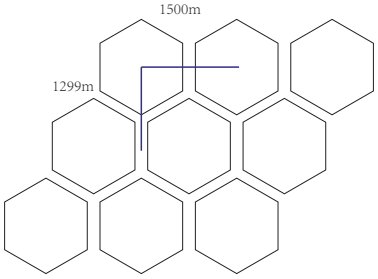

Fig. 6. 9 node scenario.

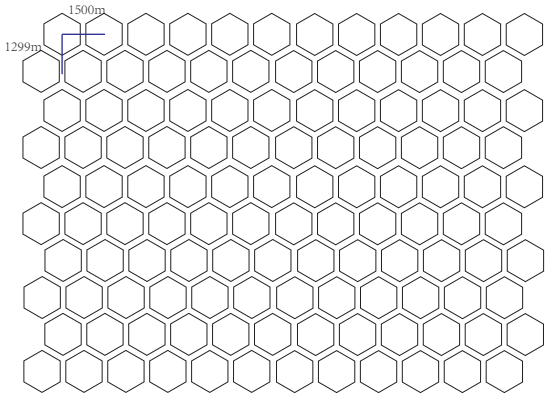

Fig. 7. 100 node scenario.

In our simulation, nodes are only sending packets to their neighbors. Each node has a constant bit rate (called UWCBR) application layer for each of its 6 neighbors: this application generates packets of 120 Bytes with a constant period of 21 seconds for the scenario with 9 nodes and 28 seconds for the scenario with 100 nodes. The total numbers of links for the two scenarios are 32 for 9 nodes and 522 for 100 nodes. The total simulation time is 35000 seconds for the 9 nodes simulation and 2100 seconds for the 100 nodes simulation. The physical

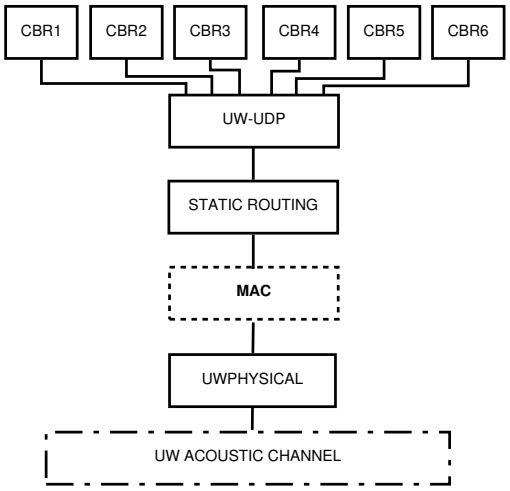

Fig. 8. Protocol stack used in the DESERT Underwater simulations.

layer (UWPHYSICAL) computes the signal to noise ratio (SNR) with the model presented in [17], while the interference model used is the DESERT MEANPOWER model, where the interference power is spread over the entire packet duration. The common simulation parameters are listed in Table IV, and the protocol stack is depicted in Figure 8: the protocol stack of a node is composed of six CBR application layers (one per neighbor), a light transport layer called UWUDP to multiplex and demultiplex the application layer packets, static routing consisting in all the nodes transmitting directly to their neighbors, one of the three MAC layers used for the evaluation, and UWPHYSICAL, the standard DESERT physical layer.

TABLE IV
COMMON SIMULATION PARAMETERS

Parameter	Value
transmission power	180 dB re uPa
propagation speed	1500 m/s
frequency	26 kHz
bandwidth	16 kHz
bit rate	1000 bps
spreading factor	2
wind speed	10
shipping	1
acquisition threshold	-3.0 dB
interference model	MEANPOWER
modulation	BPSK

B. Simulation results

In this section, we show simulation results of our two algorithms against the benchmark protocol with three performance indicators: Mean Throughput per link, Packet Delivery Ratio (PDR) and Jain's Fairness Index (JFI).

In Figure 9, we show a high improvement compared to the benchmark in terms of mean throughput per link. For the 9 nodes scenario, our 7 color solution outperforms the CSMA-Aloha 3.7 times. When the grid scales to 100 nodes, the mean throughput of CSMA-Aloha drops by 60 percent. Our 13 color scheduling still holds a high throughput per link.

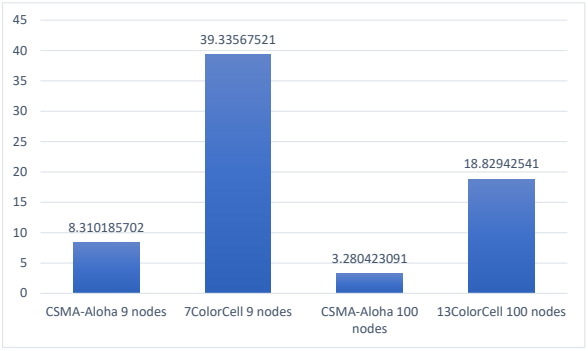

Fig. 9. Mean Throughput Per Link.

The average, standard deviation and confidence interval of the mean throughput per link computed in 20 simulation runs for both scenarios are shown in Table V

TABLE V
MEAN THROUGHPUT PER LINK

Simulation Scenario	CSMA-Aloha 9nodes	7Color 9nodes
Average	8.310185702	39.33567521
Standard Deviation	0.110742153	0.00251116
95% Confidence Interval	0.048533997	0.001100544
Simulation Scenario	CSMA-Aloha 100nodes	13Color 100nodes
Average	3.280423091	18.82942541
Standard Deviation	0.309916734	0.010078256
95% Confidence Interval	0.135824501	0.004416909

In Figure 10, we show the PDR for our solution and CSMA-Aloha. As we expected CSMA-Aloha have a lower PDR than our proposed solution. Even though we do not use a long guard time to avoid collisions like in traditional TDMA, we are able to guarantee an acceptable packet delivery ratio. As the grid scales, 7 colors would not provide a high PDR when the traffic increases. Our 13 color solution can provide a packet delivery ratio of more than 52% under full traffic load. This means that we need more control over interference when the scale of the grid becomes larger, accounting for cumulative multihop interference. The average, standard deviation and confidence interval of PDR computed in 20 simulation runs for both scenarios are shown in Table VI.

TABLE VI
PACKET DELIVERY RATIO

Simulation Scenario	CSMA-Aloha 9nodes	7Color 9nodes
Average	0.181535729	0.843318318
Standard Deviation	0.002882625	0.0000573
95% Confidence Interval	0.001263343	0.0000251
Simulation Scenario	CSMA-Aloha 100nodes	13Color 100nodes
Average	0.065743906	0.524421443
Standard Deviation	0.001363697	0.000279322
95% Confidence Interval	0.000597655	0.000122416

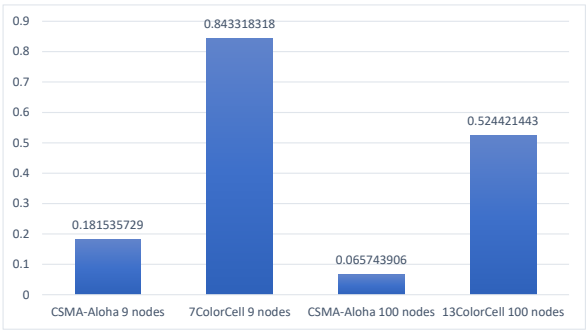

Fig. 10. Packet Delivery Ratio.

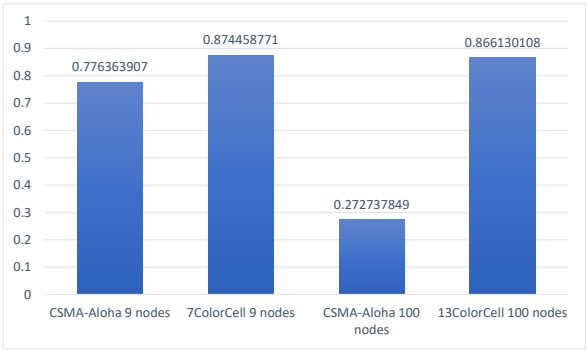

Fig. 11. Jain's Fairness Index.

In Figure 11, we show Jain's fairness index to prove that our solution achieves a good fairness. As the nodes in the center of a grid tend to suffer more interference than those at the edge, we have to examine the fairness of links to ensure our scheduling can provide all links with high throughput and packet delivery ratio.

The average, standard deviation and confidence interval of Jain's fairness index in 20 simulation runs for both scenarios are shown in Table VII.

TABLE VII
JAIN'S FAIRNESS INDEX

Simulation Scenario	**CSMA-Aloha 9nodes**	**7Color 9nodes**
Average	0.776363907	0.874458771
Standard Deviation	0.011122441	0.000001628
95% Confidence Interval	0.004874535	0.00000071
Simulation Scenario	**CSMA-Aloha 100nodes**	**13Color 100nodes**
Average	0.272737849	0.866130108
Standard Deviation	0.143726579	0.000257192
95% Confidence Interval	0.062989793	0.000112717

V. CONCLUSION AND FUTURE WORK

In this paper, we proposed a scheduling solution for large scale Underwater Acoustic Multi-hop Grid Networks. Simulation results prove our assumption about interference increase while the network scales. Our two scheduling algorithms provide improvement in throughput while keeping fairness among links. In the follow-up work, we will study more complex cell structures to mitigate interference aggregation from multi-hop grid and provide an adaptive scheduling algorithm to leverage throughput and packet loss according to the traffic and topology change.

REFERENCES

[1] I. F. Akyildiz, D. Pompili, and T. Melodia, "Underwater acoustic sensor networks: research challenges," *ELSEVIER Ad Hoc Networks*, vol. 3, no. 3, pp. 257–279, May 2005.

[2] F. Campagnaro, R. Francescon, F. Guerra, F. Favaro, P. Casari, R. Diamant, and M. Zorzi, "The DESERT underwater framework v2: Improved capabilities and extension tools," in *Proc. Ucomms*, Lerici, Italy, Sep. 2016.

[3] F. Campagnaro, F. Steinmetz, and B.-C. Renner, "Survey on low-cost underwater sensor networks: From niche applications to everyday use," *Journal of Marine Science and Engineering*, vol. 11, no. 1, January 2023. [Online]. Available: https://www.mdpi.com/2077-1312/11/1/125

[4] "Subnero M25M Series Modems," last time accessed: Apr. 2023. [Online]. Available: https://subnero.com/products/modem.html

[5] "EvoLogics Underwater Acoustic Modems," Last time accessed: Apr. 2023. [Online]. Available: https://evologics.de/acoustic-modems

[6] E. Demirors, B. G. Shankar, G. E. Santagati, and T. Melodia, "SEANet: A software-defined acoustic networking framework for reconfigurable underwater networking," in *Proc. ACM WUWNet, Washington DC, US*, Oct. 2015.

[7] R. Diamant, P. Casari, F. Campagnaro, and M. Zorzi, "Leveraging the near–far effect for improved spatial-reuse scheduling in underwater acoustic networks," *IEEE Transactions on Wireless Communications*, vol. 16, no. 3, pp. 1480–1493, March 2017.

[8] M. Chitre, M. Motani, and S. Shahabudeen, "Throughput of networks with large propagation delays," *IEEE Journal of Oceanic Engineering*, vol. 37, no. 4, pp. 645–658, October 2012.

[9] P. Anjangi and M. Chitre, "Experimental demonstration of super-TDMA: A MAC protocol exploiting large propagation delays in underwater acoustic networks," in *IEEE Third Underwater Communications and Networking Conference (UComms)*, 2016.

[10] H. Dol, "EDA-SALSA: Towards smart adaptive underwater acoustic networking," in *IEEE/MTS OCEANS 2019 - Marseille*, 2019.

[11] Y. Luo, L. Pu, M. Zuba, Z. Peng, and J.-H. Cui, "Challenges and opportunities of underwater cognitive acoustic networks," *IEEE Transactions on Emerging Topics in Computing*, vol. 2, no. 2, pp. 198–211, June 2014.

[12] A. Sgora, D. J. Vergados, D. D. Vergados, "A survey of TDMA scheduling schemes in wireless multihop networks," *ACM Comput. Surv.*, vol. 47, no. 3, apr 2015. [Online]. Available: https://doi.org/10.1145/2677955

[13] K. G. Kebkal, O. G. Kebkal, E. Glushko, L- Sebastião, A. Pascoal, J. Gomes, J. Ribeiro, H. Silva, M. Ribeiro, G. Indivery, "Underwater acoustic modems with integrated atomic clocks for one-way travel-time underwater vehicle positioning," in *Proc. UACE*, Skiathos, Greece, September 2017.

[14] "GPS NTP+PTP Network Time Server," Last time accessed: Dec. 2021. [Online]. Available: https://timemachinescorp.com/product/gps-ntpptp-network-time-server-10mz-output-tm2500/

[15] K.G. Kebkal, V. K. Kebkal, O. G. Kebkal, R. Petroccia, "Underwater acoustic modems (S2CR series) for synchronization of underwater acoustic network clocks during payload data exchange," *IEEE Journal of Oceanic Engineering*, vol. 41, no. 2, pp. 428–439, April 2016.

[16] M. DeLeon, "A study of sufficient conditions for Hamiltonian cycles," *Rose-Hulman Undergraduate Mathematics Journal*, vol. 1, no. 1, p. 6, 2000.

[17] M. Stojanovic, "On the relationship between capacity and distance in an underwater acoustic communication channel," *ACM Mobile Comput. and Commun. Review*, vol. 11, no. 4, pp. 34–43, Oct. 2007.